

Angle estimation of a robotic arm with a floating base by using low-cost IMUs

Xiaolong Zhang, Eelis Peltola, and Jouni Mattila

Abstract—An algorithm that uses low-cost inertial measurement units (IMUs) for estimating link angles for floating-base platforms is proposed. A network of low-cost IMUs for this sensor-fusion algorithm is proposed and described in detail. The error sources of our test platform are investigated.

The algorithm is validated with a commercial mobile working machine, which consist of 6 degree-of-freedom (DOF) wheeled base platform, and 3-DOF serial link hydraulic arm that forms two vertical plane 1-DOF joints to be estimated.

Although there are disturbances from the mobile machine's engine and deformation of the links themselves, the measured results obtained from the planar motion of a hydraulic arm show that the accuracy of the estimation is less than 1 degree in the criterion of theroot mean square (RMS) error.

I. INTRODUCTION

For navigation or pose estimation, strap-down microelectromechanical system (MEMS) IMUs are widely used nowadays in all kinds of mobile devices, from mobile phones to cars and more. Hydraulic manipulators with high payload capabilities also play a main role in mobile working machines: these machines can work in rough-terrain environments, such as forest machines, material transport vehicles, excavators, etc. Traditionally, joint resolvers or potentiometers are used to measure the manipulator joint angles.

In an attempt to reduce system's cost and improve robustness, the use of MEMS-based strap-down IMUs for estimating the state of manipulator joints has been investigated in [1], [2]. However, these studies assume the base of the manipulator is stationary (or fixed based). Recently, [3] developed an algorithm for pose estimation of arms with the floating base; one high quality IMU is applied to each link, and the IMUs cost more than 1000 USD each. In [4], a tactical-grade fiber optic 6-DOF IMU (KVH1750), costing >15 000 USD each, was used as an accurate reference point for a network of low-cost MEMS gyros for arm pose estimation, and therefore high-cost accurate base state IMU was required.

In [1]–[3], a forward kinematic model with data flow from previous links is used. This makes the algorithm complex, and any imperfect estimation for the state of previous links or base will propagate to the end of the links.

The pose estimation using a fusion of IMUs and other sensors, such as cameras [5], magnetometers [6] and ultra-wide

band systems [7], has been studied widely, our approach has the advantage of using only one kind of sensor chip, resulting in easier implementation and more robust final system. Most other sensors, particularly cameras, also significantly raise the cost of the system and decrease the applicability and system robustness.

The aim of the current paper is to develop an algorithm with low-cost IMUs for the state estimation of robotic arms mounted on a floating base and to remove the need to use traditional forward kinematic model. In [8], we validated our algorithm with low-cost IMUs on a three-links hydraulic arm and the rotation of lift joint simulate a base motion, and we estimate the angle of tilt joint, the result of error's RMS is 0.202 degree. But the base only had one DOF, and no disturbances caused by machine' engine excited vibration were present and real floating-base 6-DOF wheel-platform.

The proposed algorithm for the estimation of link angles is using MEMS 3-DOF IMUs (Bosch BMI160) that cost less than 5 USD each. We use four strap-down IMUs mounted on each link to form a single virtual IMU whose body-fixed frame's origin is located at the center of the joint's rotation axis. We show that the same specific force added to the joint center can be expressed in two of these fixed frames. Through algebraic manipulation of the elements of the specific force that is output from the two fixed frames, we can determine the relative angle of the two links. We then apply an Extended Kalman Filter (EKF) and a complementary filter (CF) to fuse this angle with the outputs of the gyros and estimate the accelerometer bias and drift of the gyros to decrease the noise of the proposed angle estimation.

In this paper, we validate the proposed algorithm with a heavy-duty mobile working machine, which has three-serial links that can move in a vertical plane. Tests are carried out with the base in 6-DOF motion in a rough-terrain environment. Moreover, the engine of the machine adds extra disturbances to the IMUs' measurements during the test.

The initial measured results obtained for the vertical plane motion of a hydraulic arm on floating-base show that our theory is valid, with the accuracy of the joint angle estimation within 1 degree in RMS error, which is the same order of magnitude than in studies utilizing high-cost IMUs [3].

The error analysis shows that one of the main error sources is the deformation and/or oscillation of links when external torque is added, which violates the assumption of a rigid body kinematics in our algorithm. The other error source is the high frequency disturbance caused by the machines engine, which increases the noise in the IMUs' measurements. This also increases the convergence time of

*This research work was supported in part by the Doctoral School of Industry Innovations (DSII), Tampere University of Technology (TUT), the Forum for Intelligent Machines (FIMA), and the Academy of Finland (Grant no. 294915).

Xiaolong Zhang, Eelis Peltola and Jouni Mattila are with the Department of Automation and Hydraulic Engineering, Tampere University of Technology, FI-33101, Finland. E-mail: firstname.surname@tut.fi

our algorithm.

II. THEORY BACKGROUND

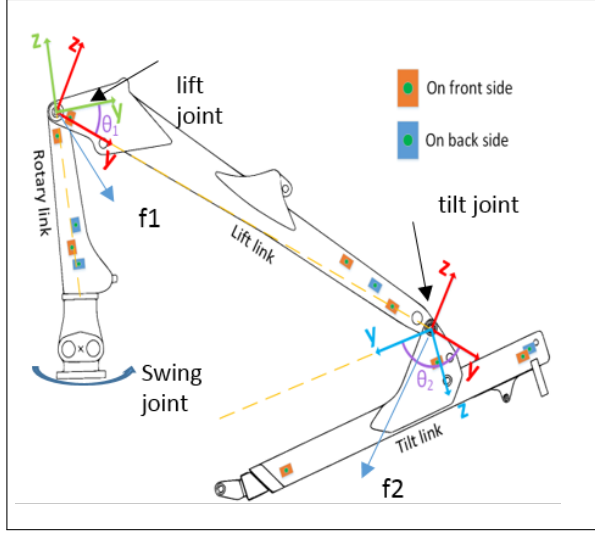


Fig. 1. 2-D chart of the hydraulic links of test platform, body-fixed frames, and IMUs boxes on the links.

A. Angle calculation with gravity-aiding

In Fig. 1, f_1 and f_2 indicate the specific forces expressed in an inertial frame, which are added in the joint center for the lift and tilt angles, respectively. Using the tilt angle as an example, we define the origins of the two body-fixed frames as being in the joint center. Also, the two x-axes coincide with the rotation axis, their y-axes are along the links, and z-axes complete the right-hand coordinate system. The force added in the tilt joint can be written as following:

$$f_2 = {}^I R_t {}^t f_t = {}^I R_l {}^l f_l, \quad (1)$$

where ${}^I R_t$ and ${}^I R_l$ are the rotation matrices from body fixed frames of the tilt link and lift link to the inertial frame respectively. ${}^t f_t$ and ${}^l f_l$ are the specific forces with respect to the inertial frame, but expressed in the body fixed frames of the tilt and lift links, respectively. From (1) we can derive the following:

$${}^t f_t = {}^I R_t^T {}^I R_l {}^l f_l, \quad (2)$$

and the rotation matrix from the body-fixed frame of the lift link to tilt link is the following:

$${}^t R_l = {}^I R_t^T {}^I R_l = \begin{bmatrix} 1 & 0 & 0 \\ 0 & \cos \theta_2 & -\sin \theta_2 \\ 0 & \sin \theta_2 & \cos \theta_2 \end{bmatrix}. \quad (3)$$

From (2) and (3), we get the following joint angle:

$$\theta_2 = \text{atan2}(f_{ty}f_{lz} - f_{tz}f_{ly}, f_{ly}f_{ty} + f_{tz}f_{lz}), \quad (4)$$

where $\text{atan2}(\cdot, \cdot)$ is the function that returns the four-quadrant inverse tangent function of the two inputs, and

f_{ty} , f_{lz} , f_{tz} , and f_{ly} are the scalar elements of ${}^t f_t$ and ${}^l f_l$ in y-axis and z-axis. It is well known that the specific force is the gravity plus the motion force. Assume two IMUs can be installed in the tilt joint center, but their coordinates are aligned with the body-fixed frame of the joined links. The outputs of the installed IMUs' accelerometers are the following:

$${}^t f_t = g_t + a_t + n, \quad (5)$$

$${}^l f_l = g_l + a_l + n, \quad (6)$$

where g_t and g_l are gravity expressed in the body-fixed frames of the tilt and lift links, respectively. a_t and a_l are the motion accelerations of the tilt-joint center expressed in the same body-fixed frames. n is the Gaussian noise of the accelerometers. From (4)-(6), we notice that once the specific force of the joint center has a projection in the motion plane of the links, the joint angle can be calculated through the output of the accelerometers.

B. Gyroscope Free IMU (GFIMU)

In practice, it is impossible to install IMUs exactly on the joint's center. We introduce the approach of gyroscope free IMUs (GFIMUs). GFIMUs use four 3-axis accelerometers that are attached on a rigid body to get the specific force, angular acceleration, and quadratic form of the angular rate on any point of the body; details can be found in [9], [10]. Through GFIMU, we can form a virtual IMU mounted in the rotation center and get rid of the forward kinematic model that is applied to the state estimation of serial links. It is also relatively easy for us to choose the positions of IMUs on the platform's links, as shown in Fig. 1, where the squares with dots indicate the IMUs boxes on links.

$$T = CF \quad (7)$$

where

$$T = \begin{bmatrix} f_{Ao} \\ {}^A \alpha_A \\ qu(\omega) \end{bmatrix}. \quad (8)$$

In (8), f_{Ao} indicates the specific force at the joint center of link A expressed in the frame of link A, ${}^A \alpha_A$ is the angular acceleration of link A expressed in the frame of link A, and

$$qu(\omega) = \begin{bmatrix} \omega_1^2 \\ \omega_2^2 \\ \omega_3^2 \\ \omega_1\omega_2 \\ \omega_1\omega_3 \\ \omega_2\omega_3 \end{bmatrix} \quad (9)$$

(9) is the quadratic form of the angular rate for link A, expressed in link A. In (7), F is the measurement of the four IMUs' accelerometers, and C is a constant matrix, which only contains the position information of the four IMUs on link A. Details can be found in [9] and III-B.

C. Data fusion

[9] developed the model for an EKF which fuses the output of GFIMUs to estimate the bias of the accelerometers and drift of the gyroscopes. The state vector contains 18 elements as follows:

$$x[k] = \begin{bmatrix} \omega[k] \\ b_g[k] \\ b_a[k] \end{bmatrix}, \quad (10)$$

where $[\omega]$ is the angular rate of one link in time step k , $b_g[k]$ is the drift of the gyroscope, and $b_a[k]$ is the bias of four accelerometers with a triad-axis. The process model is as follows:

$$x[k+1] = Ax[k] + B\tilde{F}[k] + w[k], \quad (11)$$

where the state transition matrix is as follows:

$$A = \begin{bmatrix} I & 0 & C_a\Delta t \\ 0 & e^{-D(\beta_g)\Delta t} & 0 \\ 0 & 0 & e^{-D(\beta_a)\Delta t} \end{bmatrix} \quad (12)$$

and the input matrix is as follows:

$$B = \begin{bmatrix} C_a\Delta t \\ 0 \\ 0 \end{bmatrix}. \quad (13)$$

The matrix of noise for the states is as follows:

$$w[k] = \begin{bmatrix} C_a\Delta t\eta_a[k] \\ \eta_{b_g}[k] \\ \eta_{b_a}[k] \end{bmatrix}, \quad (13)$$

where Δt is the sampling interval; C_a is a constant matrix and the part that corresponds to the angular acceleration in matrix C of (7); η_a represents the white noise of the accelerometers and is a 12 by 1 vector; η_{b_g} represents the white noise for the random walk of b_g and is a 3 by 1 vector and η_{b_a} is the white noise for the random walk of b_a and is a 12 by 1 vector. In (11), the specific force from (7) is denoted as \tilde{F} and can be regarded as a control input. The bias and drift, b_a, b_g , model as first-order Gauss-Markov random walk, in (12) the $D(\beta_a)$ represents a 12 by 12 diagonal matrix, with the element of time constant as β_a on the main diagonal. Similarly, $D(\beta_g)$ is a 3 by 3 matrix.

The observation model has a nonlinear form as follows:

$$z[k] = \begin{bmatrix} \omega[k] - b_g[k] \\ qu(\omega[k]) - C_{qu(\omega)}b_a[k] \end{bmatrix} + \begin{bmatrix} -\eta_{b_g}[k] \\ -C_{qu(\omega)}\eta_{b_a}[k] \end{bmatrix}. \quad (14)$$

The measurement is the average of the outputs of the gyroscopes on the link and the quadratic form of the angular rate from (9). We apply one EKF developed above for four IMUs mounted on each link. For every time step, the estimated bias of accelerometers, b_a , is used to correct the specific force for the joint center of each link, and (4) is used to determine the relative angle of the two links, θ .

D. Complementary filter

The angle θ has with high noise, and we use a complementary filter to smooth it.

$$\begin{bmatrix} \hat{\theta}(k) \\ \hat{b}^x(k) \end{bmatrix} = \begin{bmatrix} 1 & \Delta t \\ 0 & 1 \end{bmatrix} \begin{bmatrix} \hat{\theta}(k-1) \\ \hat{b}^x(k-1) \end{bmatrix} + \begin{bmatrix} \Delta t & 0.5\Delta t^2 \\ 0 & \Delta t \end{bmatrix} \begin{bmatrix} k_p \\ k_I \end{bmatrix} (x_2 - \hat{\theta}(k-1)) + \begin{bmatrix} \Delta t \\ 0 \end{bmatrix} x_1, \quad (15)$$

where measurement x_2 is the joint angle from (4), and $x_1 = \omega_B - \omega_A$ is the difference of the angular velocity from the output of EKF for the gyroscope's x-axis. $\hat{\theta}(k)$ and $\hat{b}^x(k)$ are the estimated angle and bias.

The estimation process for the joint angles is summarized in Fig. 2.

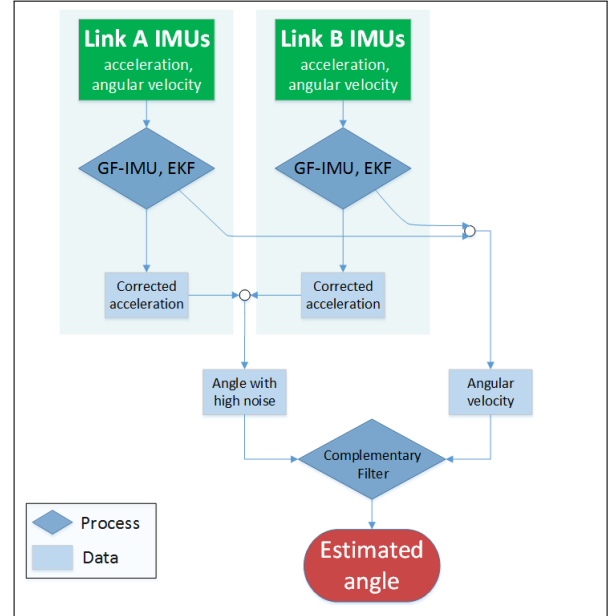


Fig. 2. Flowchart of processing for the joint angle estimation

III. EXPERIMENTS

A. Experimental setup

The Ponsse Caribou is a 12-ton, 8-wheel forest forwarder used to load and carry logs, as shown in Fig 3. It includes a typical four-link heavy-duty hydraulic manipulator arm. The first three 1-DOF joints are revolute, and the last joint is prismatic, effectively making the last link an extension. This extension link was not regarded in our setup, bringing the effective outreach of the arm to 5.5 meters. Our naming convention for the used links is seen in Fig. 1. The forest forwarder acts as a floating base for the arm.

For the algorithms in this paper, each measured joint angle needs four IMUs mounted on the links connected to that joint. We are approximating that there are two joint angles connected in series, which means that the total number of IMUs needed is 12, as shown in Fig. 1. The placement of the IMUs was chosen first by hand using educated guesses and then verified with an algorithm described in III-B.



Fig. 3. The forest forwarder that acts as our mobile test platform, complete with manipulator arm.

B. Position of IMUs on links

It is well known that the specific force on any point of a rigid body can be written as the following:

$$f_{Ai} = f_{Ao} + {}^A\omega_A \times ({}^A\omega_A \times r_{Ai}) + {}^A\alpha_A \times r_{Ai}, \quad (16)$$

where f_{Ai} denotes the specific force of the i^{th} point on link A, which has the coordinate r_{Ai} . f_{Ao} is the specific force in the origin of body frame A, ${}^A\omega_A$ is the angular rate of link A, and ${}^A\alpha_A$ is the angular acceleration; all of these are expressed in body-fixed frame A.

With (16), to get a linear expression, ${}^A\omega_A$ is written as its quadratic form, $[\omega_1^2 \ \omega_2^2 \ \omega_3^2]^T$ and $[\omega_1\omega_2 \ \omega_1\omega_3 \ \omega_2\omega_3]^T$. Regard these two vectors as two unknowns and f_{Ao} , ${}^A\alpha_A$ as the other two unknowns. If we have the values of the specific forces for four points on link A, we can extract the coordinates information into a matrix D :

$$F = DT, \quad (17)$$

where T has the same meaning and form as in (7), F is a 12 by 1 vector that stacks the specific forces of four points, and D is the following:

$$D = \begin{bmatrix} D_1 \\ \vdots \\ D_4 \end{bmatrix}. \quad (18)$$

In (18), each element of D has a form of the following:

$$D_i = [I \quad -S(r_{Ai}) \quad L(r_{Ai})], \quad (19)$$

where $S(\cdot)$ is the following skew-symmetric matrix. L is also a function of the coordinate r_{Ai} .

$$L(r_{Ai}) = \begin{bmatrix} 0 & -r1 & -r1 & r2 & r3 & 0 \\ -r2 & 0 & -r2 & r1 & 0 & r3 \\ -r3 & -r3 & 0 & 0 & r1 & r2 \end{bmatrix} \quad (20)$$

Inverse matrix D , we get matrix C in (7). We assume all the IMUs in our tests are of the same quality, and the standard deviation of their Gaussian noises are on the same level. Multiply C with its transpose, as follows:

$$W = CC^T. \quad (21)$$

Denote the diagonal elements of W as N , which is applied as the criterion for choosing the positions of IMUs on links. With (21) and (7), we notice that the first three elements in N use the measurements of the accelerometers of the IMUs to get the specific force in the joint center, the next three elements for the angular acceleration, and the last six elements for the quadratic form of angular rate.

In practice, the placements cannot be chosen freely, because hydraulic manipulator links have uneven surfaces, pipes and hydraulic hoses that come in the way of mounting. We try to keep the first three numbers of N smaller than 2 when choosing the position of the four IMUs on one link, which means the diagonal elements of the covariance matrix for the specific force in the joint center is two times larger than the measurements of the IMUs' accelerometers. Similarly, keep the other elements of N smaller than 100, meaning the standard deviation of noise for angular acceleration and quadratic form of angular rate in T is 10 times less than that of accelerometers'.

The final placements for the IMUs are provided in Table I. The choices for IMUs' positions are not optimal, but ones that are acceptable for the test results, while also being convenient for us to attach the IMUs on the platform's links.

TABLE I
IMU POSITION COORDINATES

	IMU #	Coordinates [x, y, z] (m)		
Swing link	1	-0.142	0.057	-0.642
IMUs in	2	-0.143	-0.030	-0.934
reference to	3	0.141	-0.015	-0.185
link joint	4	0.142	0.046	-0.860
Lift link	1	0.082	0.093	0.001
IMUs in	2	0.035	2.934	0.051
reference to	3	-0.243	3.047	-0.009
link joint	4	0.032	3.154	-0.044
	IMU #	Coordinates [x, y, z] (m)		
Lift link	1	0.082	-3.411	0.001
IMUs in	2	0.035	-0.570	0.051
reference to	3	-0.243	-0.457	-0.009
tilt joint	4	0.032	-0.350	-0.044
Tilt link	1	0.020	-0.650	0.498
IMUs in	2	-0.223	-0.622	0.372
reference to	3	0.075	0.112	0.138
tilt joint	4	0.020	0.972	0.525

C. Sensor implementation

MEMS technology has enabled cheap and small inertial sensors, resulting in ubiquitous use and availability, for example, [11]–[13]. In this setup, the low-cost MEMS IMU used was a Bosch BMI160 6-DOF IMU, featuring a three axis accelerometer and three axis gyroscope, at a market price of less than four euros. This results in the use of four

low-cost IMUs on one link being considerably cheaper than using one high-cost IMU, as in [2]. Each IMU was implemented in a sturdy IP66-protected box with the following hardware:

- Bosch BMI160 IMU development shuttleboard, featuring the BMI160 IMU and BMM150 magnetometer. The magnetometer was not used because metallic bodies interfere with it, making it unreliable. The BMI160 accelerometer range was configured to $\pm 8 g$, and the gyroscope range to $\pm 125 \frac{\text{deg}}{\text{s}}$. Both are given in 16-bit resolution by the BMI160.
- ARM Cortex M4 -powered STM32F407 Discovery microcontroller development board. Used for reading the IMU through a serial peripheral interface (SPI), and sending the read data forward to a computer with a Ethernet user datagram protocol (UDP). Programmed graphically in Simulink with the Waijung third-party blockset, which compiles the Simulink model to STM32F407-compatible C code.
- A custom-designed base board, hosting the aforementioned boards, a power regulator, an Ethernet physical layer (PHY) chip, and other electronics needed to support the Ethernet connection.

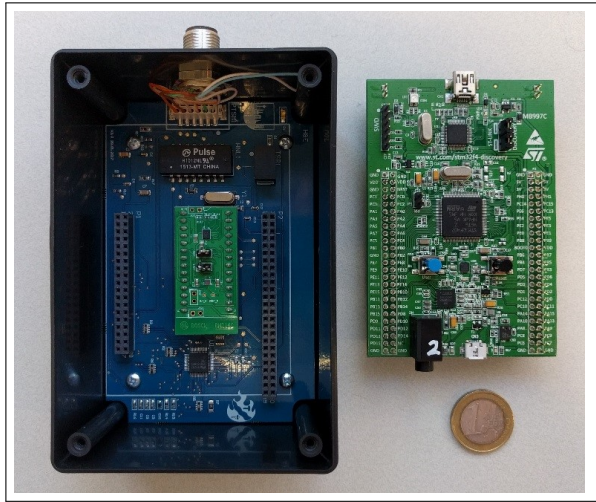


Fig. 4. The electronics used. BMI160 shuttleboard on the bigger base board, and the STM32F407 development board taken out of the box.

The electronics are pictured in a plastic box in Fig.4. The actual black BMI160 chip, with a width of 3 mm, can be seen slightly above the center on its shuttleboard. The same M12 connectors pictured are used in our metallic boxes. Each IMU sent a total of 12 bytes of raw data (two for each axis, six axes in total) at a rate of 1600 Hz. Data from the IMUs were first sent to a Simulink Real-Time target computer, where it was gathered into a single vector for each time step and sent forward. This was done purely because the dSpace MicroAutoBox II prototyping unit, which was used for data acquisition and controlling the manipulator, does not support enough UDP connections for our experiment. The Simulink Real-Time target computer sent the vector to the MicroAutoBox II, which read the incoming vectors at

a rate of 800 Hz, disregarding and dropping every other packet of the BMI160 data. Because the algorithms used in this paper were run with data rates of 400 Hz, a simple averaging of neighboring data points was done to the 800 Hz of data to get a final data rate of 400 Hz. For reference regarding the IMU data, both estimated joints also had a Heidenhain ROD 456 incremental encoder with a resolution of 5000 sine waves fixed on them. The encoders had 10-fold and 25-fold interpolation units in the lift and tilt joints, respectively, resulting in a resolution of 0.0072 degrees for the lift joint and 0.0029 degrees for the tilt joint. The encoders were read with the MicroAutoBox II to get the same time stamps for both the IMU and encoder data, ensuring precisely timed references.

IV. TEST RESULTS

TABLE II
TEST RESULTS

	standard deviation	mean abs. error	maximum error
tilt(deg)	0.947	0.612	4.49
lift(deg)	0.638	0.480	1.952

In Table II, we summarize the results of one general test for the algorithm we propose in this paper. The angles' measurements from encoders are set as references; the standard deviation, mean of absolute error, and maximum of absolute error are listed. They are counted from the first time step to the end of the test. The prior states for the EKF use zeros, and a zero for the prior value of \hat{b}^x in CF. During the test, all three joints of platform links were rotated arbitrarily in a plane by a human operator using open-loop control. The angle positions are shown at the top of Fig. 5. The mobile platform was driven several times from even ground to a slope made of rubble. This fully forms a 6-DOF platform for the hydraulic links. The base's motion is not shown in Fig. 5. The estimation error of the tilt and lift angles are shown in the middle and bottom, respectively. Because the engine of the vehicle is running at the time of testing, extra disturbance of oscillation is transferred to the links. This is analyzed in detail in IV-A. Currently, we validate the algorithm with angle estimations only for the tilt and lift joints; estimating the swing angle is our next goal.

A. Analysis of error sources

The algorithm we propose assumes all the links are rigid bodies, which means on the same link. the angular rate is the same at any point, that if the IMUs' orientations on one link are aligned, output of the angular rates should be close to each other, with the exception of some offset or drift. However, during practice tests, each link has some bending and oscillation because of external torque, and the assumption of a rigid body is not held at all times. In Fig. 6, the four plots focus on a part of the test for tilt angle estimation as the rotation angle changes at high speed. The upper left plot indicates the difference of the angular rate

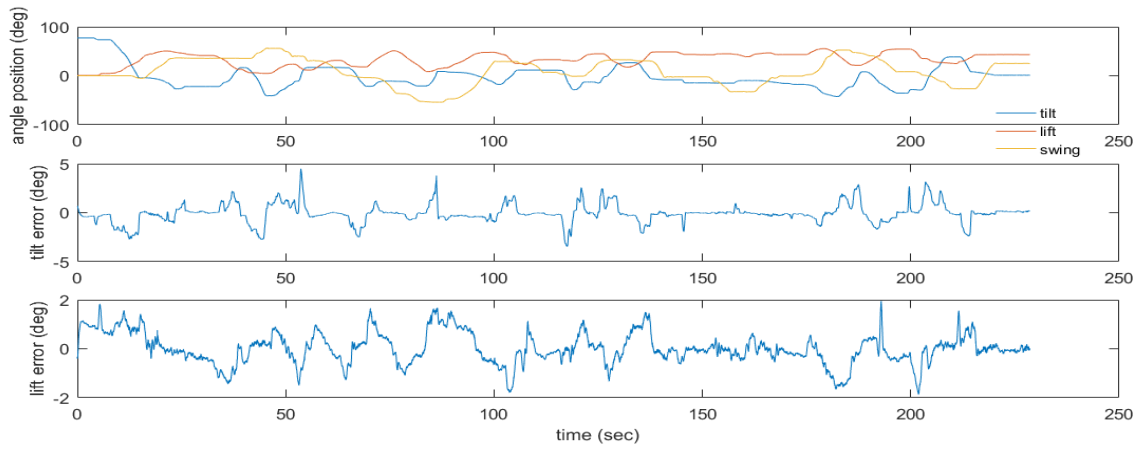


Fig. 5. The top figure shows the angle positions of the three joints; the middle one is the error of estimation for the tilt joint, and the bottom is the estimation error of the lift angle.

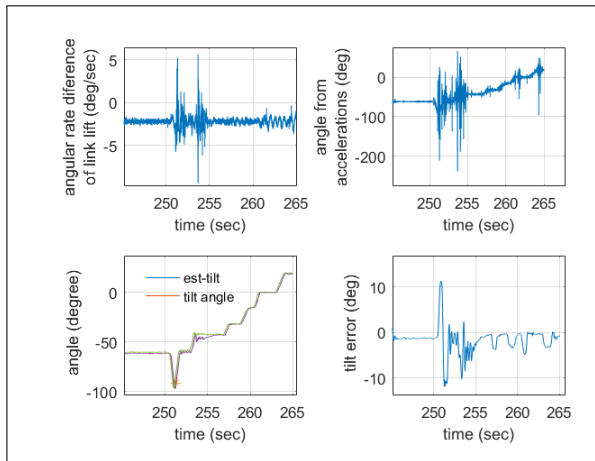


Fig. 6. Oscillation of the link itself introduces an estimation error.

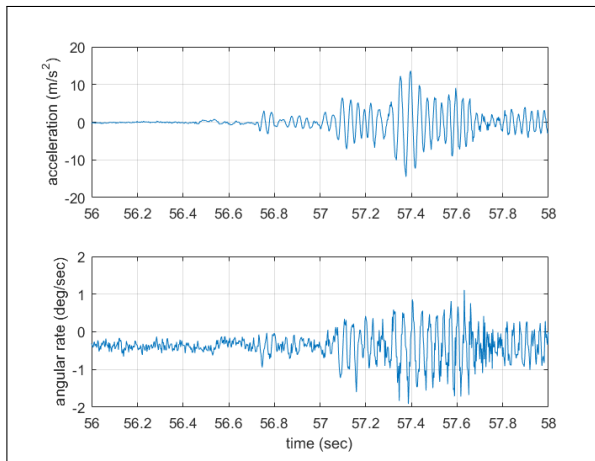


Fig. 7. Disturbances introduced to IMU by the vehicle engine.

between two IMUs on lift link in the x direction, and the peak of this difference reaches more than $5 \frac{deg}{s}$, even though the two IMUs are on the same link. The upper right plot indicates the angle value we get from equation (4): it shows that the high frequency oscillation of the link itself has a significant effect for specific force estimation on the joint's center. The bottom left plot in Fig. 6 shows the estimation result of the tilt angle: the blue line indicates the estimation result, and the red line is the output from the encoder, which is regarded as a ground truth reference. The bottom right part shows the estimation error: its peak value is about 11 degrees. This error peak occurs when the joint angle changes from -55 degrees to -95 degrees and goes back within 1 second. One of the two IMUs is located close to the link joint, and the other is close to the lift joint. The distance between them is about 3 m, so as the lift link undergoes high angular acceleration, the link's deformation or oscillation worsens the estimation.

When the engine of the test machine is turned on, the vibration of the engine will transfer to the links. As an example, the upper plot in Fig. 7 indicates the accelerometer's output of IMU number 9 in the x direction when the machine's engine is started; the bottom plot shows the gyroscope's output in the y direction for the same IMU and at the same time.

The same data for Fig. 5 are outputted in Fig. 8 in a different form, the regions of error peak, and the links stay in stationary status are enlarged. The red and dark lines indicate the encoder's measurement and estimation for the angle of lift joint, respectively. The blue and green lines are for the angle of tilt joint from encoder and its estimation. The dark star and pink star indicate the error peak of the estimation for tilt and lift angle, respectively. The angle position of swing joint and the base's motion are not shown in Fig. 8.

From the enlarged sub-boxes, we can say that the peaks of errors for angle estimation mainly occur as the joints rotate at a high speed. In this situation, the links may just have high angular acceleration, the links' deformation cause the angle estimation with (4) to become worse; although this

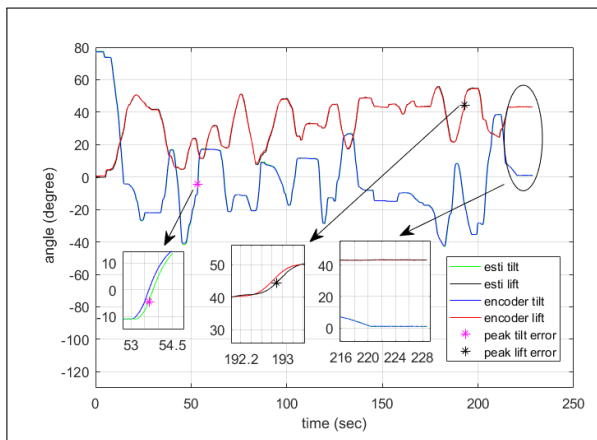


Fig. 8. The output of estimation results for tilt and lift angle, with the enlarged local regions.

deformation can recover within a very short time, but the convergence time of estimation with the CF described in (15) increase. This leads to bigger error for the final angle estimation, the shape of the estimation curve has a delay compared to the output from the encoder.

The enlarged section for the end of the estimation shows that when the links are stationary, which means the angles' positions have no motion, but the machines engine is turned on, the errors are smaller; as measured, the errors of RMS are less than 0.4 degrees for both joints.

V. DISCUSSION

In IV-A, we noticed that the non-rigid property of links introduces error for the estimation of joint angles in our algorithm. The most direct way to avoid this disadvantage is to shorten the distance between IMUs on a single link. Currently, the IMUs on the lift link are positioned so that three of them are close to the tilt joint, and the fourth is close to the lift joint. Moving the fourth IMU closer to the other three would decrease the effect of oscillation of the link itself to the angle estimation of the tilt joint angle. Alternatively, moving the other three IMUs closer to the lift joint would improve the estimation of the lift joint angle. To simplify the hardware network, we use the IMUs on the tilt link both for tilt and lift joints' angle estimation. Because choosing a longer distance between IMUs can make the elements of N smaller, choosing a distance is a trade-off for our test platform between avoiding the bending of the link affecting the measurements and having less noise when calculating the elements of T .

For the disturbances introduced by the engine shown in Fig. 7, we use (15) as a low frequency pass filter to filter the high frequency oscillation from the engine. The amplitude and frequency of the engine's disturbances also changes as engine output power changes, and this changes the time to the steady states as other disturbances added. An adaptive filter should perhaps be considered as a choice. Currently, the machine's engine is running throughout the entire test, and in (15), we set the gain, k_p and k_I , as constants 2 and 0.7, respectively.

The IMUs we use are low-cost MEMS, each of them costing less than 5 USD. We do not calibrate them before they were installed into the test environment, because calibration of the IMUs in a lab is usually expensive. One of the main aims of this work is to pursue decreasing costs for hardware.

We remove the forward kinematic model that requires a data flow between consecutive joints. The angle estimation of a joint only uses the measurement of IMUs on the two links which form the joint, that allows us to decouple the pose estimation of a robotic arm from the motion of its platform base, resulting in floating base estimation.

A. Robustness test

We usually consider the outputs of low-cost IMUs to have a bigger bias or drift than high-quality ones. By adding simulated disturbances to the raw data measured from the practice test, we can check the performance of the algorithm with some sensor are worse than specified here. For example, a simulated extra bias of accelerometers as described in (22), can be added to one of the IMUs' measurements in the test which Fig. 5 is generated from. The selected IMU is close to lift joint, and attached to the lift link.

$$\begin{cases} \Delta x = 0.3 + 0.3\sin(0.06\pi t + 0.3\pi) \\ \Delta y = 0.4 + 0.4\sin(0.08\pi t + 0.4\pi) \\ \Delta z = 0.5 + 0.5\sin(0.12\pi t + 0.5\pi) \end{cases} \quad (22)$$

where Δx , Δy , and Δz are the simulated disturbances added to the raw data; t is the simulation time. The variation of these disturbances in (22) is much bigger than that of the accelerometers' bias in this work. The EKF in the proposed algorithm is used to estimate the specific force in the center of the tilt joint, with the extra bias added to the IMU and without it. The difference of this specific force are shown in Fig. 9.

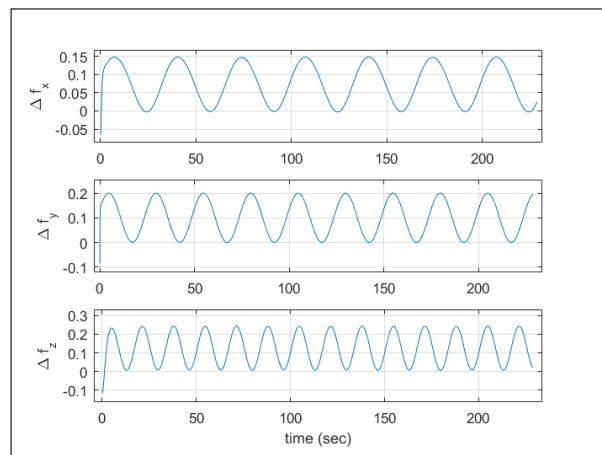


Fig. 9. Difference of specific forces in the tilt joint center.

From Fig. 9, we notice that the force's difference has the same frequency and phase as defined by (22), but the amplitude and mean values shrink to about 25% of it. If we add similar simulated bias to each accelerometer with each axis on the link lift, this difference of specific force has the same shape as the sum of the extra bias added to

each accelerometer in each axis, but amplitude decreases by about 75%. (7) and the process model of the proposed EKF have linear form and should thus hold the property of linear superposition.

There exist inaccuracies in the installation of IMUs: the orientation errors of the IMUs are about 1 or 2 degrees, and the coordinate errors are about 1 or 2 cm. In addition, the hydraulic manipulators might not move in an exact plane, and the triad-axes of the accelerometers are misaligned because we use low-cost IMUs. So except the measurement noise and bias of the IMUs measurements, there are some other errors are introduced. We use the state of the accelerometers bias, b_a , to absorb all these errors.

Similar, add disturbances to the angular rate for observation of the EKF, set the amplitude up to $5 \frac{deg}{s}$ in each direction, the differences of the estimation for specific force in joint centers is smaller than one order of magnitude compared to the noise of the forces. This means it has little effect in the output of angle calculation with (4), even if the drift of the gyroscope cannot be estimated well by the EKF. Thus, we can set the covariance of the gyroscope's noise smaller than specified, and eliminate the drift or bias for the gyroscopes in CF.

VI. CONCLUSIONS

The proposed algorithm uses the measurements of four accelerometers mounted on each manipulator link to calculate the link's angular acceleration and the specific force at the coordinate's origin. These estimates are then fused with gyroscope measurements by utilizing a complementary filter to obtain the desired joint angle estimate. We validated our algorithm in a full-scale rough terrain vehicle with the base moving with six degrees of freedom.

The novelty of the developed algorithm is that the use of a forward kinematic model requiring data flow between consecutive joints is not needed. It is validated with a heavy duty machine that has a base is in 6-DOF motion, and with three-link planar arm in 2-D motion.

Even with very low-cost IMUs (costing less than 5 USD each), without any precalibration of these IMUs and with the base of the manipulator moving over complex terrain, the accuracy of the joints' angle estimation is better than 1 degree (RMS).

As a next step, we plan to try to estimate the relative rotation angle between the platform base and the manipulator in situations where the base is not parallel with the ground or is in accelerative motion.

ACKNOWLEDGMENT

We would like to thank doctoral student Pauli Mustalahti for his help in setting up the Ponsse dSpace platform and for being allowed to use his existing code for commanding the manipulator and reading the encoders.

REFERENCES

- [1] J. Koivumäki, J. Honkakorpi, J. Vihonen, and J. Mattila, "Hydraulic manipulator virtual decomposition control with performance analysis using low-cost mems sensors," in *Advanced Intelligent Mechatronics (AIM), 2014 IEEE/ASME International Conference on*. IEEE, 2014, pp. 910–917.
- [2] J. Vihonen, J. Honkakorpi, J. Tuominen, J. Mattila, and A. Visa, "Linear accelerometers and rate gyros for rotary joint angle estimation of heavy-duty mobile manipulators using forward kinematic modeling," *IEEE/ASME Transactions on Mechatronics*, vol. 21, no. 3, pp. 1765–1774, jun 2016.
- [3] J. Vihonen, J. Mattila, and A. Visa, "Joint-space kinematic model for gravity-referenced joint angle estimation of heavy-duty manipulators," in *IEEE Transactions on Instrumentation and Measurement*. IEEE, 2017.
- [4] X. Xinjilefu, S. Feng, and C. G. Atkeson, "A distributed mems gyro network for joint velocity estimation," in *Robotics and Automation (ICRA), 2016 IEEE International Conference on*. IEEE, 2016, pp. 1879–1884.
- [5] Y. Tao, H. Hu, and H. Zhou, "Integration of vision and inertial sensors for 3d arm motion tracking in home-based rehabilitation," *The International Journal of Robotics Research*, vol. 26, no. 6, pp. 607–624, 2007. [Online]. Available: <http://dx.doi.org/10.1177/0278364907079278>
- [6] A. M. Sabatini, "Quaternion-based extended kalman filter for determining orientation by inertial and magnetic sensing," *IEEE Transactions on Biomedical Engineering*, vol. 53, no. 7, pp. 1346–1356, July 2006.
- [7] J. A. Corrales, F. A. Candelas, and F. Torres, "Hybrid tracking of human operators using imu/uwb data fusion by a kalman filter," in *2008 3rd ACM/IEEE International Conference on Human-Robot Interaction (HRI)*, March 2008, pp. 193–200.
- [8] Z. Xiaolong, P. Eelis, and M. Jouni, "Joint angle estimation for floating base robots utilizing mems imus," in *8th Conference on Robotics, Automation and Mechatronics (RAM), 2017 IEEE International Conference on*. IEEE, 2017.
- [9] T. Williams, A. Pahadia, M. Petovello, and G. Lachapelle, "Using an accelerometer configuration to improve the performance of a mems imu: Feasibility study with a pedestrian navigation application," in *ION GNSS*, 2009.
- [10] S. Park, C.-W. Tan, and J. Park, "A scheme for improving the performance of a gyroscope-free inertial measurement unit," *Sensors and Actuators A: Physical*, vol. 121, no. 2, pp. 410–420, 2005.
- [11] M. Perlmutter and S. Breit, "The future of the mems inertial sensor performance, design and manufacturing," in *2016 DGON Inertial Sensors and Systems (ISS)*, sep 2016, pp. 1–12.
- [12] F. Khoshnoud and C. W. de Silva, "Recent advances in mems sensor technology-mechanical applications," *IEEE Instrumentation Measurement Magazine*, vol. 15, no. 2, pp. 14–24, apr 2012.
- [13] A. Purwar, D. U. Jeong, and W. Y. Chung, "Activity monitoring from real-time triaxial accelerometer data using sensor network," in *2007 International Conference on Control, Automation and Systems*, oct 2007, pp. 2402–2406.